Benchmarking and measuring photodarkening in Yb doped fibers

J. Koponen*[a], M. Laurila[a], M. Söderlund[b], J.J. Montiel i Ponsoda[b], and A. Iho[b]
[a]nLIGHT Corporation, Sorronrinne 9, 08500 Lohja, Finland
[b]Helsinki University of Technology, Tietotie 3, 02150 Espoo, Finland

ABSTRACT

Photodarkening is a detrimental phenomenon known to affect ytterbium doped fibers. Methods to study the spectral and temporal properties of the photodarkening induced loss were developed. The spectral shape of the photodarkening loss measured from multiple aluminosilicate samples indicate that visible wavelength(s) could be used in benchmarking fibers for their PD induced loss. Two principal methods, core and cladding pumping, were introduced to induce a known and repeatable inversion to fiber samples. The photodarkening rate could be parameterized using a single variable, inversion. More generally, the photodarkening rate was found to follow a simple power law and to be proportional to $[Yb^*]^{7\pm1}$ (the excited state Yb ion density). Two methods, stretched exponential and bi-exponential, were used to fit the rate measurements. Both fitting methods were found suitable, with the bi-exponential method having more potential in increasing the understanding of the mechanism(s) behind photodarkening. Coiling induced spatial changes in the inversion and subsequent photodarkening performance were demonstrated for a large-mode-area fiber laser.

Keywords: Photodarkening, ytterbium, measurement, large-mode-area, mode crunching

1. INTRODUCTION

Photodarkening (PD) is a detrimental phenomenon known to affect ytterbium (Yb) doped fibers. PD of Yb doped glass can be differentiated from other degradation mechanisms by a broad spectral absorption that extends from visible wavelengths to the IR, and the characteristic temporal increase of the induced loss over time. PD can decrease the output power performance of Yb fiber lasers and amplifiers, and can for example increase the pump power requirement or decrease the lifetime of a device. The first published observation of PD of Yb doped glass was likely the unsaturated absorption reported in 1997 by Paschotta *et al.* [1], and the systematic documented study of the phenomenon started in 2005 [2].

The first objective in our PD study was to develop a PD benchmarking method for Yb doped fibers. In order to fulfill these requirements, the measurement should be fast, easy to implement, and reproducible. The core pumping method is illustrated in Fig. 1a. A typical core pumping sample was a short piece of single-mode fiber (4-6 μm core diameter with NA of 0.14 to 0.2, length approximately 10 cm), coupled to a white light source and a single-mode pump operating near the 976 nm peak absorption wavelength. The sample could be first measured for spectral transmission using the white light source and the spectrum analyzer. The fiber was then exposed to pump light for some predetermined duration (for example 30 minutes), and then again measured for the spectral transmission. The PD induced excess loss can be calculated from the measured spectra. Typical induced excess loss spectra from such measurements are shown in Fig. 2a. The induced loss is shown to be greater at the visible wavelengths, but with a significant (yet noisy) absorption at the Yb^{3+} emission wavelengths between 1000 and 1100 nm. Approximately 20 different aluminosilicate Yb fiber types were pumped to various degrees of PD, and the resulting spectra studied in particular for the ratio of PD induced at the signal wavelengths (1040-1070 nm) and a visible wavelength of 633 nm. The visible reference wavelength of 633 nm was chosen for convenience, as HeNe sources are readily available as probe sources if required. The resulting induced losses at 633 nm and signal wavelength are plotted in Fig. 2b. The measurements at the signal wavelength have a lower signal to noise ratio than the corresponding measurements made at the 633 nm. The slope of the curve shows that on average the PD induced loss at 633 nm was approximately 71 times higher than at the signal wavelength. It also suggests that the spectral response of the induced loss is stable enough for the probe wavelength to be used for benchmarking the loss at the signal wavelength.

* joona.koponen@liekki.com; phone +358 19 357 391; fax +358 19 357 3949; www.nlight.net

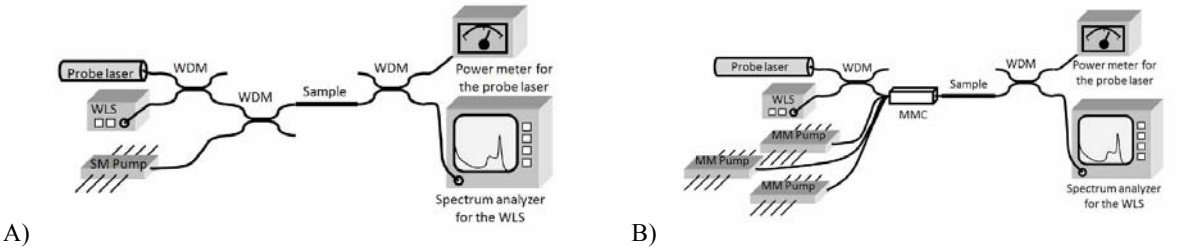

Fig. 1. Measurement setups for benchmarking and studying PD. A) Single-mode fiber setup with core propagating pump. B) Setup for double clad fibers with cladding propagating pump. In both cases sample transmission can be measured before and after photodarkening. Probe laser can be substituted with an incoherent light source with spectral filtering for convenient probe wavelength tuning. WLS = White Light Source. WDM = Wavelength Division Multiplexer. MMC = Multimode Combiner.

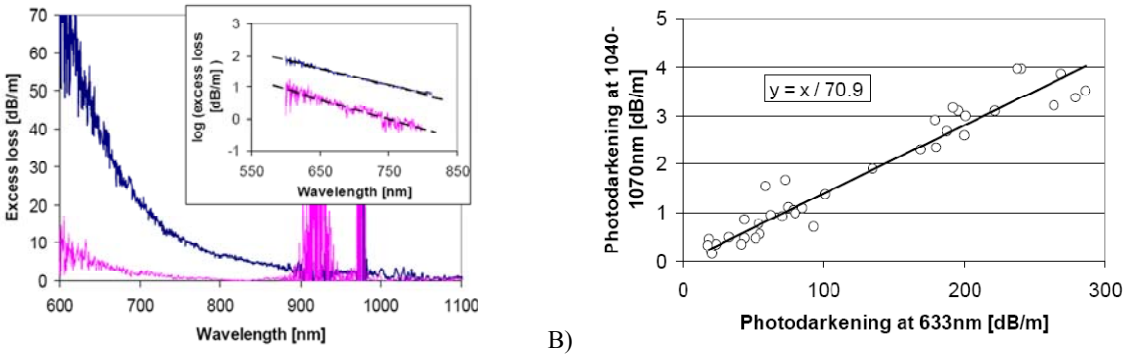

Fig. 2. Spectral behavior of PD in aluminosilicate Yb doped fibers. A) Induced excess loss examples. Inset showing linear response over a limited wavelength range in log scale. B) Correlation between induced PD at 633 nm and at Yb signal wavelength. Approximately 20 different fiber samples were measured to varying degrees of PD. The average induced photodarkening loss at 633 nm was approximately 71 times higher than at the signal wavelength.

The core pumping method was found to work well only for small core diameter fibers [3]. For large-mode-area (LMA) fibers a different method of inducing a repeatable inversion was required, and the cladding pumping method, shown in Fig. 1b was developed [4]. The measurement setup enabled a tunable inversion by changing the coupled pump power, while maintaining a flat inversion level in the longitudinal direction.

The study of the mechanism behind PD of Yb doped fibers has gotten significant interest from many research groups. The mechanism(s) behind PD remain controversial. However, several possibilities have been presented. Yoo *et al.* [5] used a CW 488 nm light source to induce excess loss in doped aluminosilicate fibers and observed a spectroscopic peak at 220 nm, which was attributed to Yb-associated oxygen deficiency centers (ODC). Based on comparisons with measurements on Yb-free fiber samples, it was suggested that these centers could act as precursors of PD in Yb-doped aluminosilicate fibers. Engholm *et al.* presented convincing results supporting the formation of Yb^{2+} ions in the glass matrix from Yb^{3+} through a charge transfer process, resulting in free holes that can act as precursors for color centers [6,7]. Observations suggesting a process involving interaction of Yb^{3+}-Yb^{3+} ion pairs or even more complicated ion clusters and subsequent formation of Yb^{2+} ions was suggested by Guzman Chávez *et al.* [8]. There have also been indications that fibers with lower Al and/or higher Yb concentrations exhibited increased PD [9,10], whereas Yb-doped phosphosilicate fibers, which are known to provide high solubility to Yb ions and thus exhibit less clustering, showed greater PD resistance [11]. Previous work has also shown the PD process to be either partially or fully reversible in many cases. Methods used to bleach PD have included temperature annealing [12], exposure to UV and visible light [8,13], and oxygen loading [5]. Recently PD has also been reported to be bleached by the pump power itself [14].

An extended description of the work presented in this paper, and a more complete list of references can be found in [15].

2. INVERSION IN SAMPLE FIBERS

Inversion is a key variable in PD measurements, as the rate of PD is highly dependent on the inversion. The two approaches, core pumping and cladding pumping (Fig. 1), were studied with simulations to find out the principal strengths and limitations of the two methods [3].

The inversion simulations described below were done using the Liekki Application Designer v4.0, using the supplied cross sectional data for aluminosilicate ytterbium fibers. Common parameters used in all the simulations were Yb ion density of 1.2×10^{26} m^{-3} and an excited ion lifetime of 0.85 ms. The amplified spontaneous emission (ASE) was calculated for 101 wavelengths between 1000 and 1100 nm, and the inversion was calculated for 100 points along the longitudinal axis, regardless of fiber length. More detailed information about the simulator and the underlying rate equations are found in [3,16]. The results presented here are simulations, assuming that the model correlates well with experiments. Data simulated with the same methods was earlier found to properly fit the experiments by Farrow *et al.* [17], and work to increase the simulation and input parameter accuracy has been on-going [18].

The objective in PD measurements is often to achieve a flat and repeatable inversion in order to have the measurement represent the whole sample volume, and to obtain repeatability for the results. In the following results, the inversion within a fiber sample is considered flat, if the standard deviation of the inversion is <1%-unit. This limit is within reach of both the core and cladding pumping methods, as shown below.

2.1 Inversion induced with the core pumping method

A range of sample lengths and pump wavelengths were simulated for a 250 mW pump power coupled to the fundamental mode of the 4 µm diameter single-mode fiber with typical Yb related parameters. The resulting average inversions levels are shown in Fig. 3, where each data point represents the average inversion with the given sample length and pump wavelength. All the simulated samples had a flat inversion, excluding the long samples pumped near the 920 nm wavelength, where also the average inversion levels are lower than the surrounding points. Higher inversion is obtained at 920 nm pumping in comparison to 976 nm pumping, however, even the 976 nm case yields an inversion of approximately 45%.

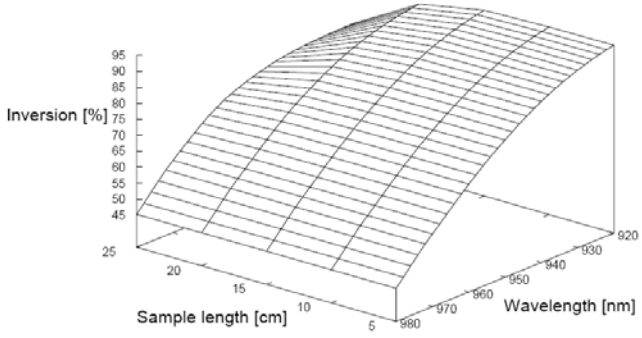

Fig. 3. Simulated average inversion in 4 µm core diameter fiber with varying sample lengths and pump wavelengths. Longer samples with shorter pump wavelengths are out of the saturated regime, and exhibit a longitudinally varying inversion. Other data points have a longitudinally flat inversion profile.

The average inversion (and corresponding standard deviation of inversion) for a 10 cm sample of single-mode 4 µm fiber as a function of coupled pump power is shown in Fig. 4. The pump irradiance is very high due to the small mode field area, and the inversion tends to saturate to the level defined by the absorption and emission cross sections (and shown in Fig. 3). The level of inversion obtained is not a function of coupled pump power above the inversion saturation threshold.

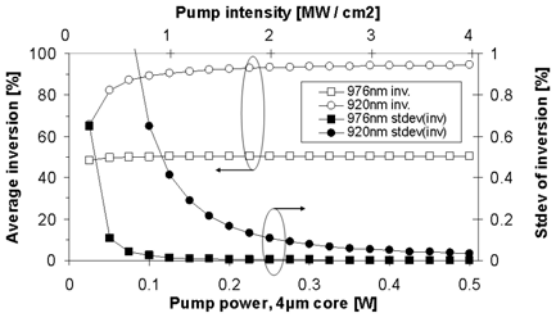

Fig. 4. Simulated average inversion in a 10 cm single-mode 4 µm diameter sample with two pump wavelengths.

The drawback of the core pumping method is the high pump irradiance required to saturate the inversion. The coupled pump power required to saturate core pumped waveguides of different diameters are shown in Fig. 5 for two pump wavelengths. The saturation threshold is defined as the minimum coupled pump power when the standard deviation of inversion in the 10 cm fiber sample is less than 1%. With for example a 300 mW pump power the maximum core diameter for 920 nm pumping is shown to be ~7 µm, and for 976 nm pumping to be ~14 µm. The core pumping method is thus most suitable for smaller core diameters.

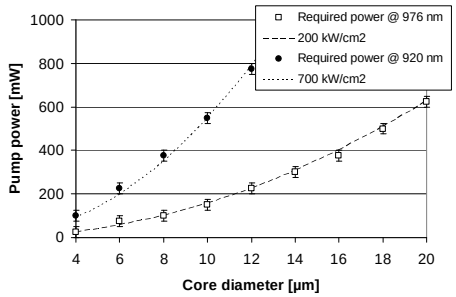

Fig. 5. Minimum pump power required to saturate the inversion of a 10 cm fiber sample in the core pumping case.

2.2 Inversion induced with the cladding pumping method

A range of sample lengths and pump wavelengths were simulated for a 20 µm core and 400 µm cladding fiber with the typical Yb related parameters, and a cladding pump power of 5 W. The resulting average inversion levels are shown in Fig. 6, where inversion in each data point was considered flat. The average inversion is seen to exhibit a shape similar to the absorption cross section. Due to this, the induced inversion is more sensitive to the applied wavelength near the 976 nm peak than at the 920 nm region.

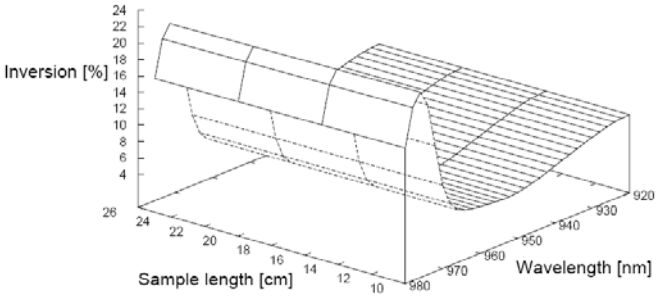

Fig. 6. Simulated inversion induced by the cladding pumping method with 5 W of coupled pump power and 20 µm / 400 µm diameter core / cladding fiber. Inversion in each data point is longitudinally flat.

The pump power inversion dependency was simulated for the cladding pumped case for the same 20/400 fiber geometry. The average inversion and the standard deviation of inversion are shown in Fig. 7. For all applied pump powers, the

inversion was flat. However, the inversion was pump power dependent. This was due to the low brightness of the pump. During cladding pumping the pump intensity (upper x-axis in Figs. 4 and 7) is in our example 100-1000 times lower in comparison to the core pumped case. Due to this, the inversion is not saturated in the cladding pumping case, and by only varying the pump power the inversion can be controlled. The pump wavelength uncertainty to the induced inversion is low if the 920 nm pumping is used. With 976 nm pumping, the pump wavelength needs to be well known and controlled.

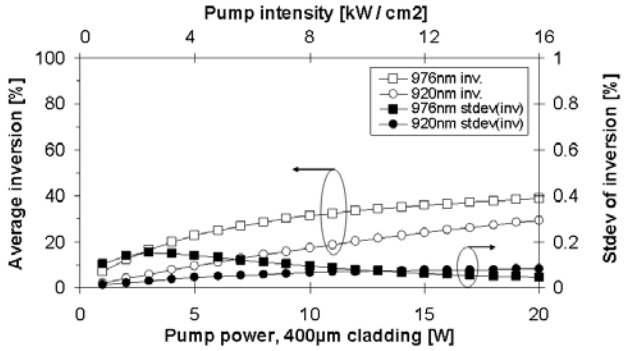

Fig. 7. Simulated inversion of a 10 cm cladding pumped sample with 20 µm core and 400 µm cladding diameters.

3. RATE OF PHOTODARKENING

Our key hypothesis in the time domain measurements was that the PD rate is driven by the inversion level of the fiber sample. The hypothesis was based on the observation that by fully inverting the fiber under test the rate of PD was no longer dependent on the pump intensity [19], which one would not expect from for example a multi-photon absorption process [20,21]. The rate inversion dependency hypothesis also supported the observations of different PD rates for different applications, while using the same or similar fiber.

The rate of PD was measured using a cladding pumping setup similar to Fig. 1 b. The transmitted power of a HeNe probe laser propagating in the core was measured at various pump power (and induced inversion) levels. The measurement results were first fitted using a stretched exponential function, and subsequently with a bi-exponential function.

3.1 Data interpretation with the stretched exponential function

Stretched exponential function was earlier used successfully in PD studies of Tm^{3+} fibers [22]. The time t dependent transmission T can be written as:

$$T(t) = A\exp\left[-\left(\frac{t}{\tau}\right)^{\beta}\right] + (1-A), \qquad (1)$$

where *(1-A)* is the steady state transmission, β is the stretch parameter ($0 \le \beta \le 1$), and τ is the PD time constant for each measurement. Within the accuracy of our measurements, the *(1-A)* value of each fit performed to the same fiber draw was constant, and the same β value was used for fiber samples of the same batch and draw. The least-square-fit method gave parameters of $\beta = 0.675$, $A = 0.99$ for Fiber #1, and $\beta = 0.65$, $A = 0.98$ for Fiber #2 with good agreement between the measurement and the fit. The measured probe transmissions are shown in Fig. 8, and examples of fit data are shown in the inset.

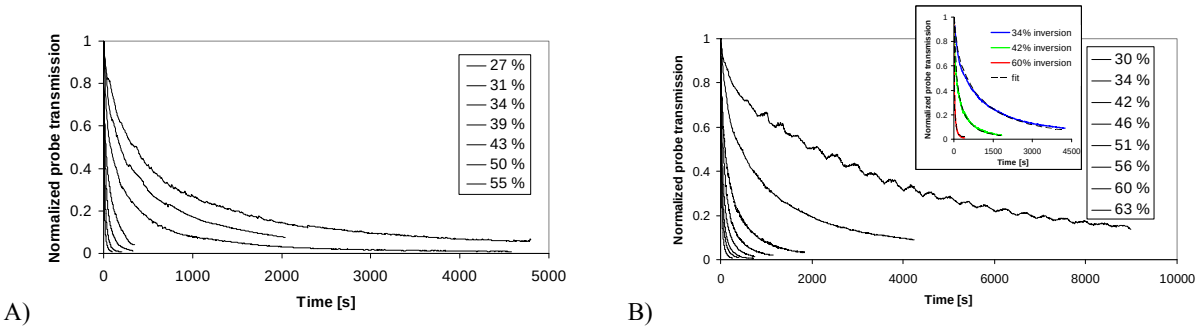

A) B)

Fig. 8. Measured normalized probe transmission for different inversion levels. A) Fiber #1. B) Fiber #2. Inset shows fit data.

The obtained time constants are plotted with their corresponding inversions in Fig. 9 a for both fiber #1 and #2. The log-log scale was chosen to highlight the PD rate inversion dependency:

$$\frac{1}{\tau} \propto I^n \Rightarrow \log\left(\frac{1}{\tau}\right) \propto n \log(I), \qquad (2)$$

where n is the slope of the linear fit, and I is inversion. For both fibers the slope was approximately seven, corresponding to a seventh power inversion dependency for the PD rate.

Both fibers #1 and #2 were of similar aluminosilicate glass, but with different Yb concentrations. The data shown in Fig. 9 a can be re-plotted as a function of the Yb excited-state number density [Yb*], which is the inversion multiplied by the Yb concentration, as shown in Fig. 9 b. By using the excited state number density as the x-axis the results for the two fibers are identical within experimental error. The result implies that, for the glass composition of these fibers, the initial PD rate is determined exclusively by the number density of excited Yb ions, not by Yb concentration or pump level, with a seventh-order dependence on [Yb*].

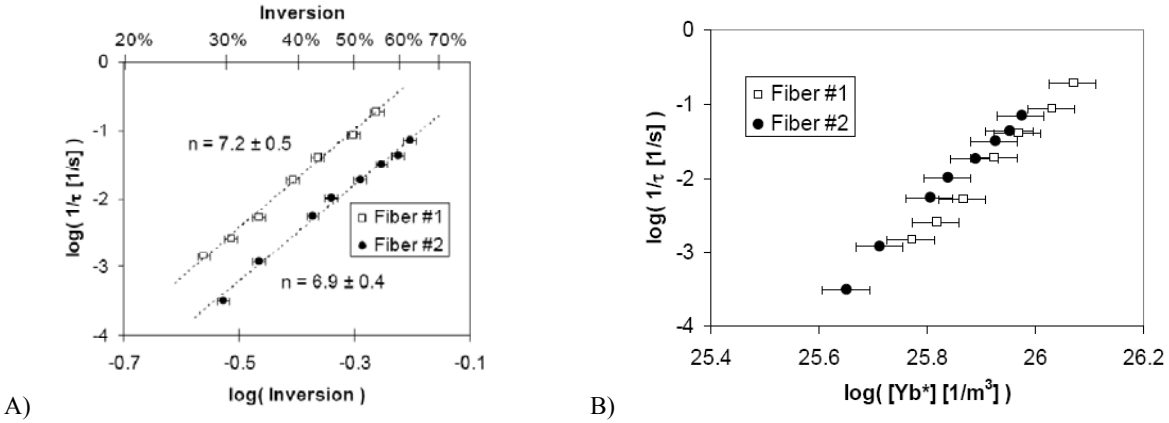

A) B)

Fig. 9. Measured PD rate constants analyzed using the stretched exponential method. A) Rate constants plotted as a function of the inversion. B) Rate constants plotted as a function of the excited state ion density, i.e. inversion multiplied with Yb ion density.

3.2 Data interpretation with the bi-exponential function

The stretched exponential function is phenomenological in the sense that although the empirical data can be fitted well, the equation is difficult to correlate to any physical phenomena. As the simple exponential fitting clearly did not work, and the stretched exponential function had drawbacks, a function was derived to fit the transmission loss induced by color centers formed by multiple paths, each path exhibiting an exponential time dependence [4]. Using this approach, the measured normalized probe light intensity $I_{norm}(t)$ could be written as

$$I_{norm}(t) = C_1(e^{-C_2(1-C_3e^{-C_4t}-(1-C_3)e^{-C_5t})} - 1) + 1, \tag{3}$$

where

$$\begin{aligned} C_1 &= \frac{I_i f}{I_i + P}, \\ C_2 &= \sigma N_f L, \\ C_3 &= c_{1,} \\ C_4 &= 1/\tau_1, \\ C_5 &= 1/\tau_2, \end{aligned} \tag{4}$$

where I_i is the incident probe light intensity, f is the fraction of the signal light propagating in the core, P is the residual pump light, σ is the absorption cross section of the color center, N_f is the final concentration of color centers, L is the length of the sample, c_1 is the amplitude fraction of the first exponential decay, and $\tau_{1,2}$ are the time constants for the first and second exponential decay.

Eq. (3) has five adjustable parameters, and as such obtaining a good fit to the data would not be strong evidence for the validity of this approach. However, many of the parameters in Eq. (4) can be constrained by physical arguments. We can first set $C_1 = 1$, assuming that there is no signal light propagating in the cladding, no residual pump light, and no detector offset. C_2 consists of parameters that should not vary between samples of the same fiber, and C_2 can thus be kept constant between the different measurements of the same fiber type. The same applies for C_3, which defines the relative amplitudes of the two pathways. This leaves only two adjustable parameters, C_4 and C_5, which are the two first order time constants.

The measurement data and bi-exponentially fit curves are shown in Fig. 10 for fiber #1, and Fig. 11 for fiber #2. The fitting was first done by letting C_2 and C_3 vary for each measured curve. The obtained values were approximately the same for each measurement, and the shown curves were fit by using the same values of $C_2 = 5.6$ and $C_3 = 0.15$ for each measurement.

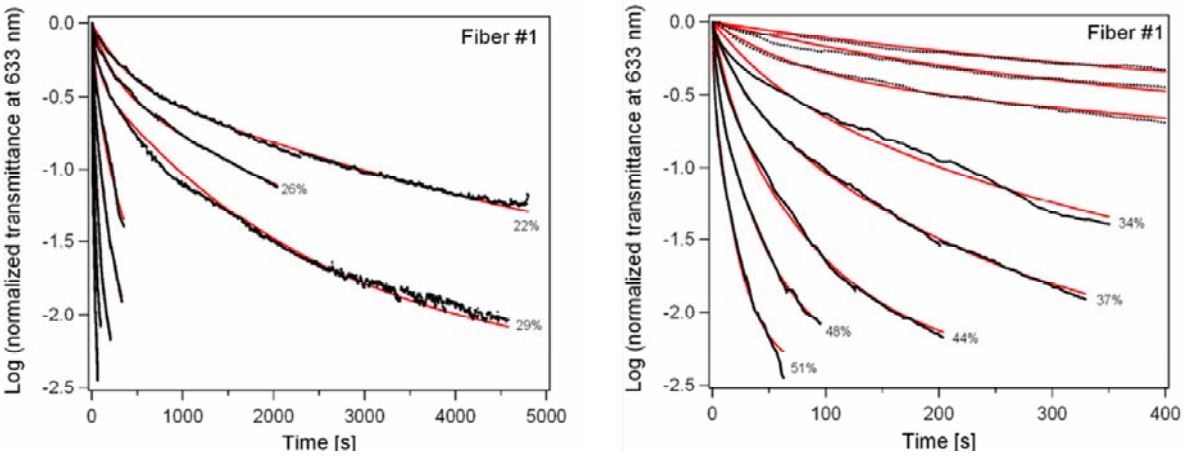

Fig. 10. Normalized 633nm probe transmittance for fiber #1. Dots = measured signal, solid curves = bi-exponential fit. The left graph shows the full measurement time, and the right graph shows the early times. Corresponding inversion levels are inserted next to the curves.

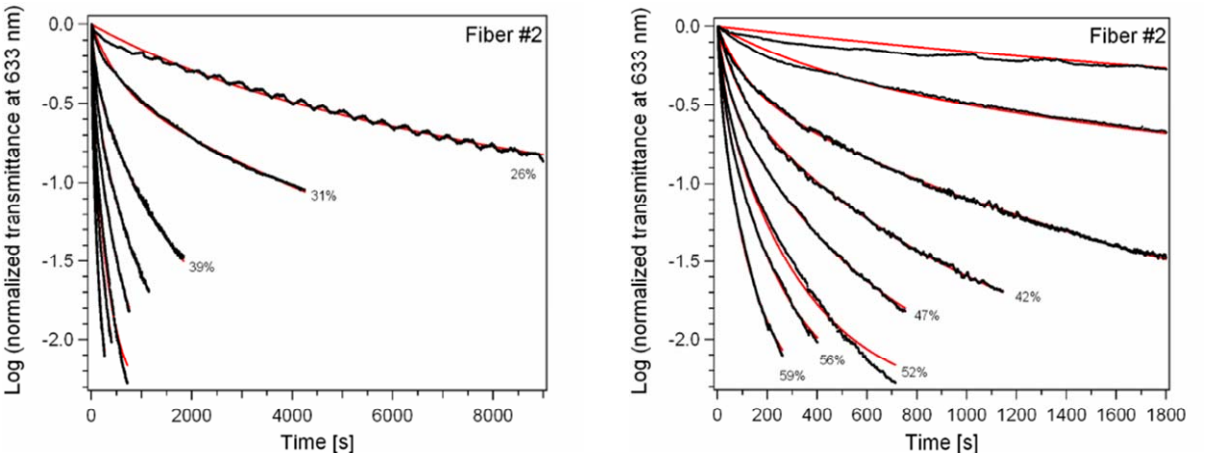

Fig. 11. Normalized 633nm probe transmittance for fiber #2. Dots = measured signal, solid curves = bi-exponential fit. The left graph shows the full measurement time, and the right graph shows the early times. Corresponding inversion levels are inserted next to the curves.

The fast and slow PD rate constants (from the fits shown in Figs. 10 and 11) are plotted as a function of inversion in Fig. 12. The error bars of inversion represent two standard deviations, and take into account the uncertainties of the simulation, namely cross section uncertainty and coupled pump power uncertainty. The linear fitting of the fast and slow PD rates resulted in slopes of ~7 for both fibers and fast/slow components. As earlier described, also the relative amplitudes of the two processes were similar for both fibers, ~4:1 in favor of the slow process.

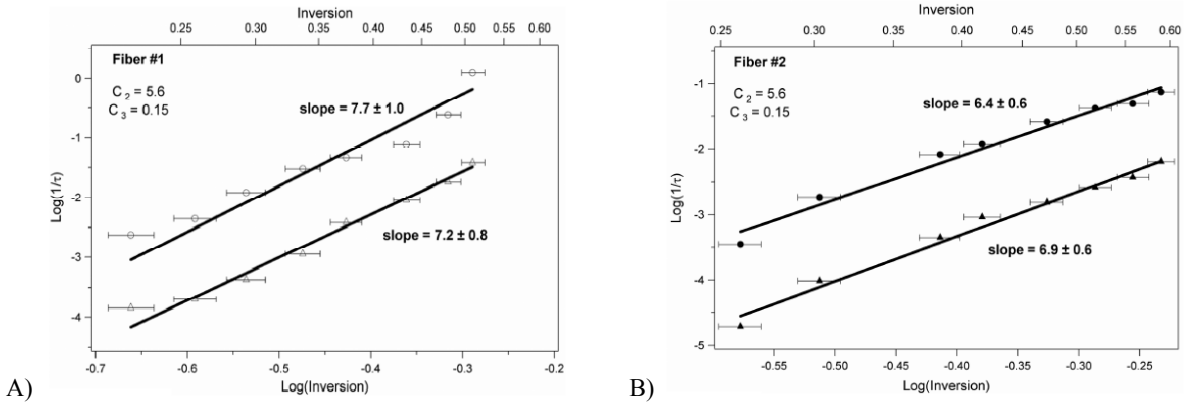

Fig. 12. Measured fast and slow PD rate constants analyzed using the biexponential method. The error bars represent two standard deviations. Symbols: round = fast rate, triangle = slow rate. A) Fiber #1 results. B) Fiber #2 results.

Similarly as was done with the stretched exponential fit, all results were scaled with the Yb ion concentration of the said sample. The PD rate constants were plotted with the resulting excited state number density of the ions, or [Yb]*, as shown in Fig. 13. The results of the two fibers agree within experimental error, indicating that the initial PD rate is proportional to the excited state number density, rather than strictly to inversion.

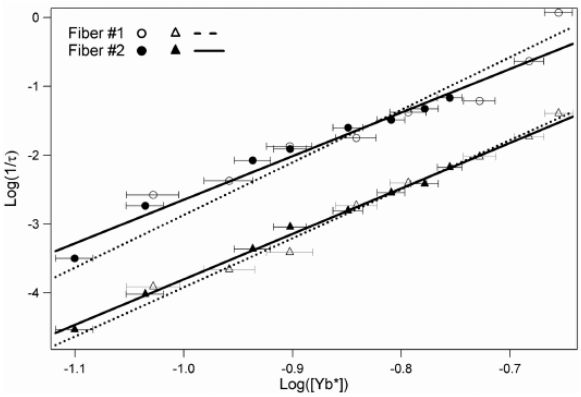

Fig. 13. Measured fast and slow PD rate constants from Fig. 12 re-plotted using the excited state number density of Yb ions as the x-axis. Symbols: round = fast rate, triangle = slow rate.

3.3 Summary of the PD rate results

The measured PD rate could be fit with both the stretched exponential method and the bi-exponential method, the latter providing potentially a more fruitful tool to further analyze the mechanism(s) behind PD. The initial PD rate results presented above consistently showed an inversion to the 7th power dependency to the initial PD rate. Subsequent studies have reported values between 4 and 6 [11,14]. The main drawback of the presented results was the short exposure time of the samples due to instabilities in the measurement. The main limiting factor was the coupled probe intensity, which was known to drift over an extended time period. To increase the measurement time to near or full PD saturation, and to increase the repeatability of the measurement, a setup was built to photodarken and to temperature bleach the same sample for multiple times [23]. The work to derive the inversion power dependency accurately is still on-going. Thermal effects during the measurements, and differences in the samples (such as material composition and manufacturing method) make direct comparison of the results between different groups challenging. The latest results highlight the importance of performing the measurements closer to the PD saturation level. A thorough report describing how measurements done with different normalized exposure times can lead to different PD inversion dependencies was recently published by Jetschke *et al.* [24].

Normalized PD time constants for systems operating on different inversion levels at two assumed inversion power dependencies are shown in Fig. 14. The figure shows the ranges of PD rates that are obtained for different operational regimes, with DC CW lasers having a very low inversion, DC amplifiers having a higher inversion, and core pumped applications having the highest inversion levels. Subsequently, the operational PD rate between CW lasers and pulsed amplifiers can exceed 3-4 orders of magnitude, and the core pumped applications operate at even higher inversion levels yielding the highest PD rate.

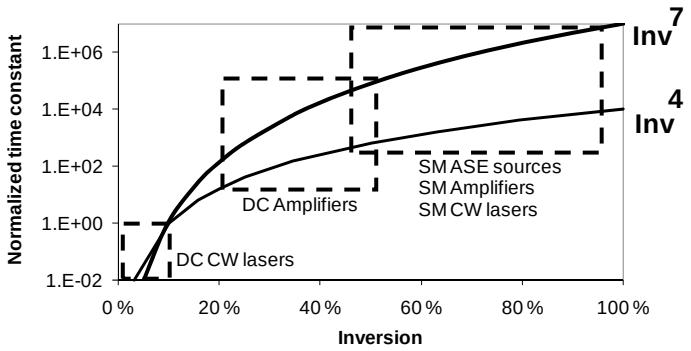

Fig. 14. Normalized PD time constants for two different inversion correlations. PD rate difference between cladding pumped CW lasers and cladding pumped amplifiers can exceed 3-4 orders of magnitude with the assumed power of four dependency.

4. COILING INDUCED SPATIAL PD CHANGES

LMA fibers are often operated while under tight coiling to increase the loss of the higher order modes, thus increasing the beam quality [25]. The coiling of the fiber causes mode crunching, i.e. the mode(s) of the fiber propagate at the outer edge of the bent waveguide. At the same time, the cross-sectional area of the (fundamental) mode is reduced. This causes the inversion of the fiber to become non uniformly distributed in the radial direction: propagating mode(s) reduce the inversion, while the volume of fiber on the inside edge of the waveguide has an elevated level of inversion. Additionally, due to the pump absorption and subsequent reduction of pump brightness, the inversion typically is longitudinally non uniform. The non-uniform inversion distribution should also affect the PD properties of the fiber. The spatial differences in PD were demonstrated roughly at the same time by simulations [26] and by using white light transmission measurements [27].

4.1 Measurement method

The measurement setup illustrated in Fig. 15 was used to study the mode crunching induced PD in a fiber laser. A fiber sample was coiled to a predetermined radius, and placed in the setup. The fiber laser consisted simply of the active fiber with 4% Fresnel reflections at each end from the cleaved fiber ends. The signal light was at approximately 1060-1080 nm with a wide emission spectrum. The laser was pumped from one end, and output power from each end was measured after the dichroic mirrors. The transmitted pump power was measured from the output end of the fiber.

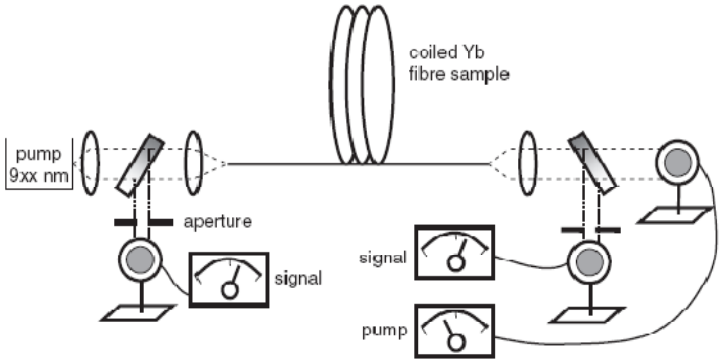

Fig. 15. Measurement setup to study mode crunching induced PD. Each active fiber was coiled and used as a cw fiber laser cavity. Signal was separated from pump using dichroic filters. Signal power from both ends of the fiber was measured, and the excess pump power out of the fiber was measured.

For each measurement the slope PCE values were calculated from the measured signal powers and the absorbed pump power. The apertures were used to filter out the signal leaked to the cladding owing to bend induced losses. To remove the effect of different coiling diameters and subsequently different losses to the modes the PCE values were all normalized to the pristine fiber samples. The PCE values of the pristine fiber samples varied between 35% (for small coiling diameters with strong leakage outside the core) to 70% (for large coiling diameters with little leakage outside the core). Each measurement consisted of the following steps:

1) Measurement of the slope PCE of a pristine fiber sample.
2) Running the laser in CW operation for 180 minutes to induce PD in the highly inverted volume of the fiber.
3) Second PCE measurement to verify that the low inversion volume of the fiber had not significantly photodarkened in CW operation.
4) Recoiling of the fiber in order to bend the fiber to the opposite direction. The fiber ends were fixed to reference planes during the operation to ensure that the rotation of the fiber could be controlled (minimized).
5) Third PCE measurement to measure the PCE of the laser while the signal propagates through the part of fiber that had high inversion during the CW operation in step 2.

4.2 Results

Each LMA fiber sample had a 30 µm core diameter and a 250 µm octagonal cladding diameter. The core and cladding NAs were 0.07 and 0.46 NA, respectively. The coiling diameter of the sample fibers was varied from 47 to 160 mm. The sample lengths were chosen to be 2 m for the 976 nm pump wavelength, and 3 m for the 920 nm pump wavelength, resulting in 8-10 dB pump absorptions for the samples.

The results of experiments are shown in Fig. 16. The error of each normalized PCE result was estimated to be ± 3%-units, mainly resulting from the unrepeatability of the measurement (fiber endface quality from cleaving and pump coupling uncertainty due to alignment). As the results show, very little or no degradation is observed in the 160 mm and 100 mm coiling diameter cases. With the smallest coiling diameter of 47 mm the fiber is shown not to degrade (within experimental error) in the CW operation, but during the third PCE measurement after re-coiling the efficiency is decreased. For samples #1 and #3 the measurements were performed by using two different pump wavelengths. The results, shown in Fig. 16 b, show similar performance regardless of pump wavelength. Sample #2 did not show a similar behavior. We suspect this was due to spatially few-moded lasing and subsequent decrease in inversion level.

A)

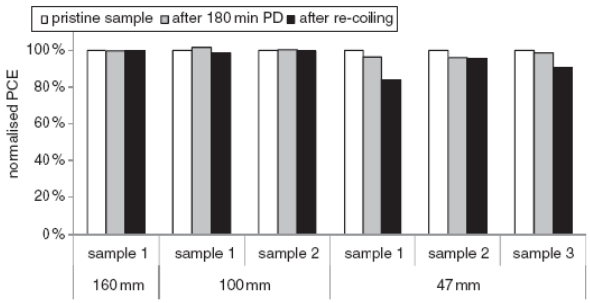

B)

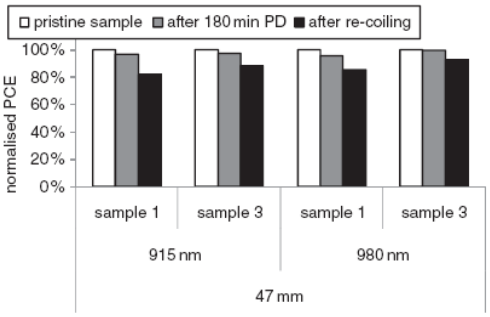

Fig. 16. Measurement results. Normalized PCE with pristine fiber, after cw lasing, and cw lasing after re-coiling and bending of the fiber to force the beam to propagate in the part of fiber formerly in higher inversion. Clear bending induced PD results were obtained only with the smaller coiling diameter of 47 mm. A) All coiling diameters. B) Smallest coiling diameter of 47 mm with two pump wavelength.

The simulated fundamental mode beam profiles inside the coiled fibers are shown in Fig. 17. Simulations were performed using the Liekki Application Designer v3.3. The smallest coiling diameter shows significant mode crunching, leaving the dark part of the fiber in high inversion, which supports the experimental results. During the experiments, the only method used to suppress higher-order modes was the one-directional coiling. Because of this, the lasing in the cavity may have been spatially few-moded, which would partially suppress the inversion in the region shown as dark in Fig. 17. In a case of strictly single-mode operation (e.g in an amplifier with good launching conditions) we expect the effect to be more pronounced. To observe the effect, one still has to re-coil the fiber in a way that the modal overlap changes within the core. In larger diameter low NA fiber amplifiers that are coiled to near single-mode operation the effect may be of importance if the same fiber is coiled and re-coiled during experiments, and the core material of the fiber is susceptible to PD.

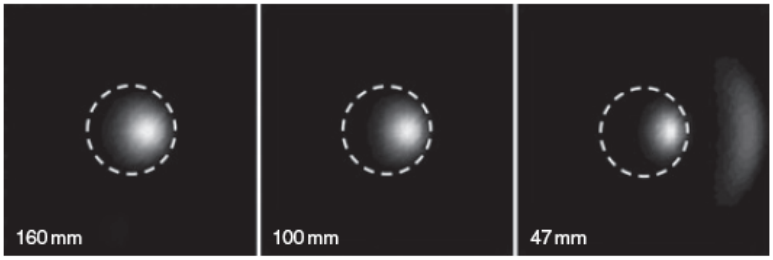

Fig. 17. Simulated intensity profile of the fundamental mode at the used coiling diameters.

5. CONCLUSIONS

The principal goal of this work was to develop a method for characterizing the PD propensity of fiber samples, and to obtain the results fast. Finding methods to study the driving mechanism behind PD became a subsequent goal of this work in order to further understand the implications of the PD in different applications.

A benchmarking measurement method was developed for single-mode fibers. The measurement method relied on inducing a flat and repeatable inversion level to the samples by saturating the inversion level. The loss measurements were conducted spectrally, and it was shown that the PD benchmarking and study could be performed at shorter wavelengths (for example the HeNe wavelength of 633 nm) to improve the signal-to-noise ratio when compared to measurements conducted at the signal wavelengths (at 1030-1100 nm).

A method to induce a flat and variable inversion to Yb doped fibers was developed in order to study the temporal behavior of PD. The measurements conducted on DC Yb doped fiber samples revealed that the key driver behind PD rate is the inversion level induced in the doped glass. Two different methods were used to analyze the decay rate data: the stretched exponential method and the bi-exponential method. The stretched exponential method gave phenomenological means of quantifying the PD rate, and the bi-exponential method enabled describing the PD rate as the result of multiple exponential decay processes. The resultant PD rate constants can be parameterized in terms of a single variable, the excited-state Yb concentration in the fiber. In addition to identifying the key controlling variable in PD, this result implies that a given glass composition can be characterized by a unique PD propensity. This propensity can be used to quantitatively compare different fibers, guide development of new fibers, and identify critical aspects of the fiber fabrication process control. Additionally, PD time constants were found to follow a simple power law. The initial PD rate measurements were proportional to $[Yb]^{*7\pm1}$, and other groups have reported dependencies ranging from power of 4 to power of 6. The results suggest that at least 4 Yb* ions in close proximity may be involved in the PD process. This very high-order dependence has significant implications for fiber devices, yielding orders of magnitude differences in the PD rate for dissimilar applications such as a cw cladding pumped lasers versus a high gain amplifier. The simple functional dependence for the PD rate on inversion may indicate a single, well-defined mechanism for color-center formation, although other physical processes cannot yet be ruled out.

The core pumping and the cladding pumping methods of inducing inversion were simulated to find the principal strengths and weaknesses of both methods. The critical parameter defining the inversion in the core pumping method was found to be the pump wavelength, assuming pump irradiance above the saturation level of inversion are used. This property makes the induced inversion very repeatable, as methods to stabilize the wavelength are readily available with for example fiber Bragg gratings. To decrease the pump power required for inversion saturation, the pump wavelengths near 976 nm absorption peak can be used. The cladding pumping method was found to have multiple critical parameters that define the inversion level: pump power, pump wavelength, and sample length all require to be controlled to induce a known and repeatable inversion. Due to the above, the core pumping method can be seen to be more suitable for benchmarking measurements, and the cladding pumping method more applicable for advanced studies of the PD phenomenon.

The radial distribution of PD was studied in an LMA fiber. The inversion simulation and white light transmission experiments were experimentally confirmed by inducing mode crunching in a CW fiber laser cavity. The mode crunching induced PD effect may be of lesser importance in commercial applications where the fiber is packaged once, and not re-coiled or handled after packaging. The effect can, however, explain repeatability problems in experimental

conditions where the same fiber may be coiled multiple times between experiments. The effect also needs to be taken into account when designing further methods of measuring PD from LMA fibers.

ACKNOWLEDGMENTS

Dr. Dahv Kliner, Dr. Jeffrey Koplow, Dr. Mircea Hotoleanu, Dr. Simo Tammela, and Dr. Hanna Hoffman are acknowledged for their contributions.

REFERENCES

[1] R. Paschotta, J. Nilsson, P.R. Barber, J.E. Caplen, A.C. Tropper, and D.C. Hanna, "Lifetime quenching in Yb-doped fibres," Opt. Comm. **136**, 375-378 (1997).

[2] J. Koponen, M. Söderlund, S. Tammela, H. Po, "Measuring photodarkening from Yb doped fibers," in Conference of Lasers and Electro-Optics / Europe, CLEO/Europe Technical Digest (OSA, 2005), paper CP2-2-THU.

[3] J. Koponen, M. Laurila, and M. Hotoleanu, "Inversion behavior in core and cladding pumped Yb-doped fiber photodarkening measurements," Applied Optics **47**, 4522-4528 (2008).

[4] J. Koponen, M. Söderlund, H. J. Hoffman, D.A.V. Kliner, J.P. Koplow, and M. Hotoleanu, "Photodarkening Rate in Yb-doped Silica Fibers," Applied Optics **47**, 1247-1256 (2008).

[5] S. Yoo, C. Basu, A. J. Boyland, C. Sones, J. Nilsson, J. K. Sahu, and D. Payne, "Photodarkening in Yb-doped aluminosilicate fibers induced by 488 nm irradiation," Opt. Lett. **32**, 1626-1628 (2007).

[6] M. Engholm, L. Norin, and D. Åberg, "Strong UV absorption and visible luminescence in ytterbium-doped aluminosilicate glass under UV excitation," Opt. Lett. **32**, 3352-3354 (2007).

[7] M. Engholm, and L. Norin, "Preventing photodarkening in ytterbium-doped high power fiber lasers; correlation to the UV transparency of the core glass," Opt. Express **16**, 1260-1268 (2008).

[8] A.D. Guzman Chávez, A.V. Kir'yanov, Yu.O. Barmenkov, and N.N. Il'ichev, "Reversible photo-darkening and resonant photobleaching of Ytterbium-doped silica fiber at in-core 977-nm and 543-nm irradiation," Laser Phys. Lett. **4**, 10, 734–739 (2007).

[9] T. Kitabayashi, M. Ikeda, M. Nakai, T. Sakai, K. Himeno, and K. Ohashi, "Population Inversion Factor Dependence of Photodarkening of Yb-doped Fibers and its Suppression by Highly Aluminum Doping," in Conference of Lasers and Electro-Optics, CLEO Technical Digest (OSA, 2006), paper OThC5.

[10] B. Morasse, S. Chatigny, E. Gagnon, C. Hovington, J-P. Martin, and J-P. de Sandro, "Low photodarkening single cladding ytterbium fiber amplifier," Proc. SPIE **6453** (2007).

[11] A.V. Shubin, M.V. Yashkov, M.A. Melkumov, S.A. Smirnov, I.A.Bufetov, and E.M.Dianov, "Photodarkening of alumosilicate and phosphosilicate Yb-doped fibers," in Conference of Lasers and Electro-Optics / Europe, CLEO/Europe Technical Digest (OSA, 2007), paper CJ3-1-THU.

[12] J. Jasapara, M. Andrejco, D. DiGiovanni, and R. Windeler, "Effect of heat and H2 gas on the photo-darkening of Yb3+ fibers," in Conference of Lasers and Electro-Optics, CLEO Technical Digest (OSA, 2006), paper CTuQ5.

[13] I. Manek-Hönninger, J. Boullet, T. Cardinal, F. Guillen, S. Ermeneux, M. Podgorski, R. Bello Doua, and F. Salin, "Photodarkening and photobleaching of an ytterbium-doped silica double-clad LMA fiber," Opt. Express **15**, 1606 (2007).

[14] S. Jetschke, S. Unger, U. Röpke, and J. Kirchhof, "Photodarkening in Yb doped fibers: experimental evidence of equilibrium states depending on the pump power," Opt. Express **15**, 14838 (2007).

[15] J. Koponen, "Measuring photodarkening from Yb doped fibers," D.Sc. dissertation, TKK Dissertations, http://lib.tkk.fi/Diss/2008/isbn9789512296682/ (2008).

[16] M. A. Rebolledo, S. Jarabo, M. Hotoleanu, M. Karasek, E. Grolmus, and E. Juanart, "Analysis of a technique to determine absolute values of the stimulated emission cross section in erbium-doped silica fibres from gain measurements," Pure Appl. Opt. **6**, 425–433 (1997).

[17] R. L. Farrow, S.W. Moore, P. E. Schrader, and A. V. Smith, "Numerical simulations of Yb^{3+}-doped, pulsed fiber amplifiers: comparison with experiment," in Conference of Lasers and Electro-Optics CLEO Technical Digest (Optical Society of America, 2008), paper CThL6.

[18] A. Iho, M. Söderlund, J.J. Montiel i Ponsoda ,J. Koponen, S. Honkanen, "Modeling inversion in an ytterbium-doped fiber," in SPIE proceedings of *Optical components and materials VI*, SPIE **7212**, 7212-08 (2009).

[19] J.J. Koponen, M.J. Söderlund, S.K. Tammela, and H. Po, "Photodarkening in ytterbium-doped silica fibers," Proc. SPIE **5990**, 599008 (2005).

[20] I. J. Booth, J. L. Archambault, and B. F. Ventrudo, "Photodegradation of near-infrared-pumped Tm3+-doped ZBLAN fiber upconversion laser," Opt. Lett. **21**, 348-350 (1996).

[21] G. R. Atkins and A. L. G. Carter, "Photodarkening in Tb3+-doped phosphosilicate and germanosilicate optical fibers", Opt. Lett. **19**, 874-876 (1994).

[22] A. Chandonnet, P. Laperle, S. LaRochelle, and R. Vallée, "Photodegradation of fluoride glass blue fiber laser," in Photosensitive Optical Materials and Devices, Mark P. Andrews, Ed., Proc. SPIE **2998**, 70 (1997).

[23] J. J. Montiel i Ponsoda, M. Söderlund, J. Koponen, A. Iho, S. Honkanen, "Combined photodarkening and thermal bleaching measurement of an ytterbium-doped fiber," in proceedings of *Fiber Lasers VI: Technology, Systems, and Applications*, Denis V. Gapontsev, Dahv A. V. Kliner, SPIE **7195**, 7195-87 (2009).

[24] S. Jetschke, U. Röpke, "Power-law dependence of the photodarkening rate constant on the inversion in Yb doped fibers," Opt. Lett. **34**, 109-111 (2009).

[25] D.A.V. Kliner, F. Di Teodoro, J.P. Koplow, S.W. Moore, and A.V. Smith, "Efficient second, third, fourth, and fifth harmonic generation of a Yb-doped fiber amplifier," Opt. Commun. **210**, 393-398 (2002).

[26] M. Hotoleanu, J. Koponen, and T. Kokki, "Spatial distribution of photodarkening in large mode area Ytterbium doped fibers," in Conference of Advanced Solid State Photonics, ASSP Technical Digest (OSA, 2008), paper WE23M.

[27] M. Söderlund, J.J. Montiel i Ponsoda, S.K.T. Tammela, K. Ylä-Jarkko, A. Salokatve, S. Honkanen, " Mode-induced transverse photodarkening loss variations in large-mode-area ytterbium doped silica fibers," Opt. Express **16**, 10633-10640 (2008).